

**ANALYSIS OF DEGRADATION AND  
EVOLUTION OF MODEL  
PARAMETERS OF a-Si/ $\mu$ -Si PV  
MODULES**

**Elif ABASLIOGLU**

**Director: Santiago SILVESTRE**

## Introduction

The combination of an amorphous silicon top cell with a microcrystalline silicon bottom cell to form a stacked tandem cell, is called micromorph cell. Micromorph tandem solar cells are considered as one of the most promising new thin-film silicon solar-cell concepts.

Tandem amorphous / microcrystalline silicon thin-film solar modules with low output voltage have gained many attentions recently. A micromorph cell is usually laser scribed into cells and the cells are series connected. In order to achieve the low output voltage, the panel needs to be additionally laser scribed into several segments and the segments are then parallel connected. The industrial relevance of micromorph solar cells improves enormously if they are combined with thin a-Si:H top cells, forming a 2-cell tandem stack in which the a-Si:H cell faces the sun. Given the large difference in the bandgap values of these two semiconductors (about 1.0 eV and 1.7 eV), a much better utilization of the solar spectrum and hence a higher PV efficiency is achieved. Importantly, because of the low short-circuit current density ( $J_{sc}$ ) of stable a-Si:H cells ( $\sim 13$  mA/cm<sup>2</sup>), the thickness of the  $\mu$ c-Si:H cell in the stack does not have to be increased significantly compared to a stand-alone  $\mu$ c-Si:H cell. Besides, micromorph solar cells tend to have open circuit voltage around 0.54 V. The micromorph tandem cells offer a wider range of the sun spectrum.

Due to the disordered nature of amorphous silicon, a-Si solar cells are subject to the Staebler-Wronski effect, which reduces the solar cell efficiency by up to 15 percent within the first months of exposure. Even though the stable  $\mu$ c-Si:H bottom cell contributes to a better stability of the entire micromorph tandem cell under light-soaking, micromorph cells show light-induced degradation (LID) too. In fact, it could be shown that the LID of the micromorph cell is due to the amorphous cell alone. Despite the fact that the concept of a micromorph solar cell brings progress via a new stable bottom cell into the thin-film silicon scenario, the stability of the amorphous silicon top cell remains still the crucial topic.

This degradation affects especially the internal parameters of the solar cell as the short circuit current, ideality factor, saturation current and series and shunt resistances. The degradation rate can be based on the comparison of the monitoring outdoor performance with the initial indoor measurements taken as references or by applying Linear Correlation Approach (LCA) and Classical Seasonal Decomposition (CSD) methods with temperature correction. The outdoor performance of micromorph modules depends also on spectral variations of the irradiance. Its relationship between seasonal variation, climatic conditions and module performance allows perception for optimized micromorph modules.

Understanding the origin of these degradation modes and how they affect the performance of PV modules is essential to improve the reliability of PV modules and to select best technology for each specific climatic condition. In this study, the behavior of micromorph PV modules under long term outdoor exposure is analyzed. The PV system is installed in Jaén (Spain, Latitude: 37° 47' 14.35" N, Longitude: 3° 46' 39.73" W, Altitude: 511 m), in a relatively dry and sunny inland site with a Continental-Mediterranean climate. The period under exposure ranges from late July 2011 to October 2014.

Furthermore, the variation of main solar cell parameters is also evaluated by means of parameter extraction techniques. A new parameter extraction procedure is carried on in order to obtain main model parameters of the solar cells forming the PV system. The parameter extraction has

the daily monitored data of the PV system in real operation of work as input and calculates the temporal evolution of main parameters.

## Methodology

The PV array output is based on five main parameters: Photocurrent  $I_{ph}$ ; diode reverse saturation current  $I_0$ ; ideality factor  $n$ ; the series and shunt resistances,  $R_s$  and  $R_{sh}$  respectively. The relationship between output current and voltage is given by the following nonlinear implicit equation:

$$I = I_{ph} - I_0 \left[ \exp\left(\frac{V+R_s I}{nVt}\right) - 1 \right] - \frac{V+R_s I}{R_{sh}}$$

### ▪ Output power of PV array

The effective peak power of a PV array,  $P^*_M$ , at STC shows dependency to irradiance and cell temperature as given by the following equation:

$$P^*_M = \frac{G^* P_{DC}}{G [1+\gamma(T_c-T_c^*)]}$$

Outdoor monitoring is subject to continuously changing operating conditions as irradiation, temperature and spectrum. The evaluation of  $P^*_M$  requires a previous filtering process for irradiance values in order to avoid the influence of operational anomalies, such as shade on the PV array, inverter saturation, inverter-off, irradiance instabilities, etc. Thus, the irradiance values for  $G < 700 \text{ W/m}^2$  are discarded.

### ▪ Power – Irradiance Method

This proposed technique is developed to determine the LID phenomenon under the real conditions of work by comparing the initial and stabilized powers at the DC output with the real measurements. The predicted initial and stabilized data values of the array power at the DC output are indicated as boundary conditions to determine the stabilization period. These values are using irradiance ( $G$ ) and module temperature ( $T_c$ ) from the real measurements as input and can be calculated with the following equations:

$$P_{DC-initial-predict} = P_{array-initial-STC} * f_{temp} * f_g * \eta$$

$$P_{DC-stabilized-predict} = P_{array-stabilized-STC} * f_{temp} * f_g * \eta$$

$$f_g = \frac{G_{measured}}{G_{STC}}$$

$$f_{temp} = (1 + kv \cdot \Delta T) \cdot (1 - ki \cdot \Delta T)$$

$$\Delta T = T_c - T_n$$

where  $P_{DC\_initial\_predict}$  is the predicted array power at the DC output (W);  $P_{array\_initial\_STC}$  is the initial peak power of PV array calculated with the initial measured data ( $\text{kW}_p$ );  $f_{temp}$  is the derating factor due to temperature correction, dimensionless;  $kv$  and  $ki$  are the voltage and current temperature coefficients respectively provided in the manufacturer's data sheet ( $1/^\circ\text{C}$ ),  $P_{DC\_stabilized\_predict}$  is the predicted array DC power (W);  $P_{array\_stabilized\_stc}$  is the peak power of PV array calculated with the data from the datasheet of the module ( $\text{kW}_p$ );  $\eta$  is the general efficiency referred to general system losses which changes between 0.84 y 0.89,  $G_{measured}$  is the real irradiance data measured by the pyranometer ( $\text{W/m}^2$ );  $G_{STC}$  and  $T_n$  is the reference irradiance under STC,  $1000 \text{ W/m}^2$  and  $25 \text{ }^\circ\text{C}$ .

Additionally, in order to analyze the degradation rate over the exposure time linear correlation approach (LCA) is used by plotting linear trend line of the measured DC array power for each month. So as to apply this approach to P-G method, trend line equation can be interpreted as:

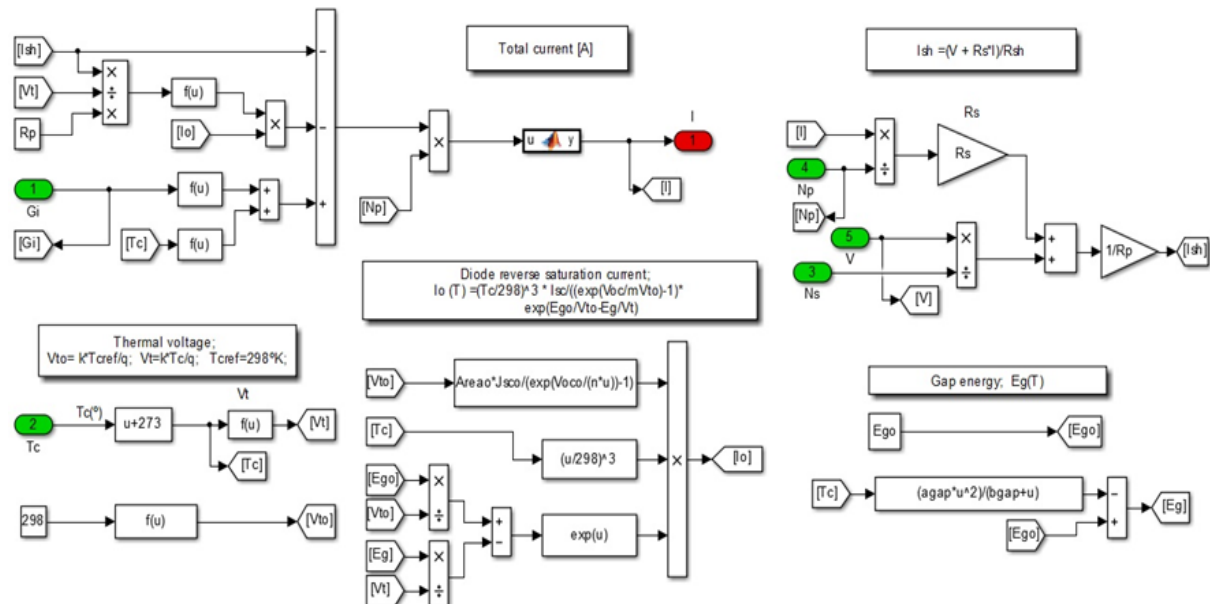
$$P_{DC-mpp} = C_G \cdot G_{measured} + A_{DC}$$

where  $P_{DC-mpp}$  is the array DC power output at the maximum power point,  $C_G$  is the gradient,  $G_{measured}$  is measured irradiance ( $W/m^2$ ) and  $A_{DC}$  is the y-intercept of  $P_{DC-mpp}$  when the irradiance is equal to zero.

### Parameter extraction

One of the objectives of this work is the analysis of the variation of the solar cell model parameters for micromorph (a-Si/ $\mu$ -Si) PV modules in real conditions of work. Therefore, this study includes parameter extraction techniques in order to find the set of solar cell model parameters to be able to reproduce the actual behavior of the whole photovoltaic system with a good accuracy degree. In order to see how these parameters affect the module performance, current – voltage and power – voltage curves are plotted by using different values of mentioned parameters. It is observed that when  $J_{sc0}$  increases, short circuit current of the cell increases too. When series resistance  $R_s$  increases, power output of the cell decreases significantly. On the other hand, varying  $R_{sh}$  and ideality factor has less effect on the cell's performance; that just makes a small change in fill factor.

The parameter extraction algorithm evaluates:  $I_{ph}$ ,  $R_s$ ,  $R_{sh}$ ,  $I_0$  and  $n$ . Daily profiles of monitored electrical parameters –namely, current and voltage at the DC output of the PV array, together with  $G$  and  $T_c$  - are used as inputs of the parameter extraction algorithm. The Simulink diagram of the algorithm are shown in the following figure.



## Results and Discussions

### Output power of PV array

In the first months of exposure a decrease of  $P^*_M$  is observed due to the LID phenomenon. The decrease occurs more slightly compared to a-Si solar cells because of the  $\mu$ c-Si layer. Also, a seasonal variation of  $P^*_M$  can be seen clearly. The initial decrease in output power of the array is followed by an increase over the summer months, a decrease over winter months and once

again an increase over summer months. The regeneration on summer months can be attributed to spectral effects, thermal regeneration and light-induced annealing.

The degradation rate calculated from the trend line of power line is  $-2.20638 \pm 0.15$  %/year. The analytical uncertainty reported along with the degradation rate was determined from the standard errors of the linear fit. The amount of LID phenomenon depends on the thickness of a-Si layer, the distribution of light, spectrum, and temperature at the specific location of the PV array.

The stabilization period was observed to start after 5 months of operation in Jaen. The trend line is obtained by sixth polynomial correlation with  $R^2$  equal to 0.9499. The stabilized level of DC output power of the array is around 640 W in the range of G and  $T_c$  considered in data filtering process. Power line demonstrates almost a constant trend after the stabilization period. Concurrently with the linear trend of the power line, a sinusoidal form attributable to the seasonal effects can also be observed. The effect of seasonal oscillation remains after the stabilization period for about 5 % variation from the stabilized level of DC power.

#### ▪ **P-G technique**

As mentioned before, in this proposed technique, two main indicators are provided as a boundary condition,  $P_{DC\_initial\_predict}$  (red) and  $P_{DC\_stabilized\_predict}$  (green). The measured DC array power is plotted and it is expected to change the tendency from the initial values to the stabilized ones in the course of time. From stamp plot of data transition of power lines, the measurement of degradation value and strength between two parameters evaluated using statistical analysis in order to provide a clearer picture of the LID phenomenon. The data transition of power lines through the magnitude gradient of power degradation per month is analyzed. The evaluation of the gradient over the total time of exposure is plotted. It shows a strong initial degradation for the first month and the decrease continues for the following 4 months. After the stabilization period which is observed as 5 months, the gradient values tend to stabilize with a slope almost equal to zero. The stabilization periods of micromorph technology is indicated as 6-8 weeks in literature. Based on the results of this technique, it can be said that even the  $\mu$ -Si solar cells are less exposed to LID phenomenon; because of thicker a-Si layers of the studied PV modules, stabilization period in this case is longer than indicated in the literature.

#### ▪ **Parameter extraction**

The higher temperatures in summer period decrease the band-gap resulting in a decrease in open-circuit voltage. The combination of band-gap reduction and strong increase of temperature in summer periods along with the increase in short circuit current due to LID effect lead to an increase of the saturation current despite the reduction of recombination effects in summer.

Another extracted solar cell parameter, short circuit current,  $I_{sc}$ , also shows a continuous decrease throughout the exposure time. After the first 5 months, it shows a more stable trend. However, a seasonal effect on  $I_{sc}$  can also be seen clearly. The improvement in output current during summer time is due to the effect of solar spectral irradiance and to thermal-recovery of the LID. The lower temperatures in winter also reduce the thermal recovery rate for the a-Si solar cells. The minimum value of  $I_{sc}$  in the worst winter months is approximately 12% less than the peak value of this parameter in the months of August. This reduction is smaller compared to a-Si results shown in the literature.

On the other hand, for the first 5 months there is a 57% of decrease in  $R_{sh}$ . After the stabilization period, shunt resistance continues to decrease but with a lower rate, 22%. As a final result, it is observed that  $R_{sh}$  reduces to 30% of its initial value. Additionally, the evolution of  $R_{sh}$  shows the same seasonal trend that the evolution of the output power of the PV array and  $I_{sc}$  as expected.

The series resistance,  $R_s$ , shows a continuing increase along the monitoring campaign. The values of  $R_s$  go from an initial value of 0,03  $\Omega$  to a final value of 0,06  $\Omega$ . The seasonal effect can be also observed in the trend of  $R_s$  that presents higher values in winter, with maximum values in the month of December, and reduced values in summer, with minimum values in the month of August.

The evolution of the ideality factor for this kind of solar cell shows seasonality like as the other extracted parameters. The evolution of  $n$  is opposite to the trend shown by the saturation current, as expected. The ideality factor shows a small reduction in summer while it increases in winter periods. However, the value of  $n$  fluctuates around a mean value of  $n = 1.2$  and the seasonal variations are small. This fact indicates that the diode included in the equivalent circuit of the solar cell corresponding to the five parameter model is dominated by the  $\mu\text{-Si:H}$  substrate (bottom cell).

## Conclusions

The degradation modes of micromorph PV modules and how they affect the performance of PV modules in a relatively dry and sunny inland site with a Continental-Mediterranean climate is analyzed in this study. The data used in this study was obtained under outdoor long term exposure of the PV system in Jaén from late July 2011 to mid-December 2014.

A reduction of the DC power of the PV array by about 12.3% was observed in the first month of outdoor deployment. The stabilization period was observed to start after 5 months of operation with a decline of the DC power by the relative percentage of 15.9 % and then it is stabilized. However, the effect of seasonal oscillation remains after the stabilization period for about 5 % variation from the stabilized level of DC power.

Solar cell parameters identification is also addressed in this study by using a parameter extraction technique. The sets of solar cell model parameters obtained by using the parameter extraction technique are able to reproduce the behavior of the PV array in real conditions of work with a good accuracy degree. The parameter extraction technique is able to evaluate the temporal evolution of main solar cell model parameters and helps to understand the evolution of the entire system at PV module level.

The seasonal variation of micromorph PV modules behaviour was also observed in the evolution of the solar cell model parameters. The evolution of each one of the model parameters along the outdoor long term exposure of the PV system has been analyzed and allows achieving a better understanding of the performance changes of the PV modules and the evolution of the output power of the PV array.